表2　再石灰化促進物質

	再石灰化物質（由来）	化学物質名	補助物質	構　造	作　用
1	糖アルコール	キシリトール ソルビトール マンニトール		OH基を複数個もつ 糖アルコール	カルシウム可溶化 エナメル質再石灰化
2	ガゼインホスフォペプチド（牛乳）	ガゼインホスフォペプチド	非結晶性リン酸カルシウム	アミノ酸残基21～25個にリン酸基4～5個結合	カルシウム吸収促進 カルシウム可溶化 エナメル質再石灰化 齲蝕抑制
3	フノリ抽出物（紅藻類フノリ）	フノラン	第2リン酸カルシウム	多糖類	カルシウム可溶化 エナメル質再石灰化
4	リン酸化オリゴ糖（馬鈴薯デンプン）	リン酸化オリゴ糖カルシウム		グルコース残基3～7個のマルトオリゴ糖にリン酸基1～2個結合	pH緩衝作用 カルシウム可溶化 エナメル質再石灰化

おわりに

スクロースの齲蝕誘発性，代用甘味料の齲蝕誘発性について考察し，食品による齲蝕予防という概念が実際に有効であるのかについて考えてきたが，糖アルコールを中心とした非齲蝕誘発性甘味料配合の食品を上手に摂取することにより齲蝕を幾分かは予防できる可能性が示されたと思われる。今後は新機能の再石灰化促進作用をもつ食品が齲蝕予防にどれだけ貢献できるか，臨床試験等での調査が期待される。

文　献

1) Newbrun E.: Current concepts of caries etiology. In Cariology, The Williams & Wilkins Co., Baltimore. 15-43, 1978.
2) 井上昌一，う蝕の疫学．「う蝕細菌の分子生物学 研究の成果と展望」，武笠英彦（監），クインテッセンス出版. 21-28, 1997.
3) Weiss RL and Trithart AH.: Between-meal eating habits and dental caries experience in preschool children. Am. J Public Health. 50: 1097-1104, 1960.
4) Stephan RM.: Effect of different types of human foods on dental health in experimental animals. J Dent Res. 45: 1551-1561, 1966.
5) Ooshima T, Izumitani A, Minami T, *et al.*: Trehalose does not induce dental caries in rats infected with mutans streptococci. Caries Res. 25: 277-282, 1991.
6) Koulourides T, Bodden R, Keller S, *et al.*: Cariogenicity of nine sugars tested with an intraoral device in man. Caries Res. 10: 427-441, 1976.
7) 今井 奨，う蝕病因論と代用甘味料によるう蝕予防．日本歯科評論. 668: 51-62, 1998.
8) Bär A.: Caries prevention with xylitol. A review of the scientific evidence. Wld Rev. Nutr. Diet. 55: 183-209, 1988.
9) van Loveren, Sugar alcohols.: What is the evidence for caries-preventive and caries-therapeutic effects? Caries Res. 38: 286-293, 2004.
10) 今井 奨，キシリトールなどの効果は？ 日本歯科評論. 63: 13-15, 2003.

J Oral Pathol Med (2004) 33: 292–9

www.blackwellmunksgaard.com/jopm

p53 gene status and expression of p53, MDM2, and $p14^{ARF}$ proteins in ameloblastomas

Hiroyuki Kumamoto[1], Takashi Izutsu[1], Kousuke Ohki[1], Nobuhiro Takahashi[2], Kiyoshi Ooya[1]

[1]Division of Oral Pathology, Department of Oral Medicine and Surgery, and [2]Division of Oral Ecology and Biochemistry, Department of Oral Biology, Tohoku University Graduate School of Dentistry, Sendai, Japan

BACKGROUND: To clarify the roles of the p53–MDM2–$p14^{ARF}$ cell cycle regulation system in oncogenesis and cytodifferentiation of odontogenic tumors, *p53* gene status and expression of p53, MDM2, and $p14^{ARF}$ proteins was analyzed in ameloblastomas as well as tooth germs.

METHODS: Paraffin sections of 16 tooth germs and 46 benign and 5 malignant ameloblastomas were examined immunohistochemically for the expression of p53, MDM2, and $p14^{ARF}$ proteins. Frozen tissue samples of 10 benign ameloblastomas and 1 malignant (metastasizing) ameloblastoma were analyzed by direct DNA sequencing to detect *p53* gene alteration.

RESULTS: Immunohistochemical reactivity for p53 was detected in 2 of 13 tooth germs, 13 of 29 ameloblastomas, and 5 of 5 malignant ameloblastomas, and the expression ratio of p53 in tooth germs was significantly lower than those in benign and malignant ameloblastomas. Direct DNA sequencing showed no alteration of *p53* gene exons 5–8 in any sample of 10 benign ameloblastomas and 1 metastasizing ameloblastoma. Expression of MDM2 and $p14^{ARF}$ was detected in all samples of normal and neoplastic odontogenic epithelium, and the expression ratios in tooth germs tended to be lower than those in benign and malignant ameloblastomas. In ameloblastomas, expression of p53, MDM2, and $p14^{ARF}$ was significantly higher in plexiform cases than in follicular cases. Markedly decreased reactivity for p53, MDM2, and $p14^{ARF}$ was detected in keratinizing and granular cells in ameloblastoma subtypes. Basal cell ameloblastoma showed slightly higher reactivity for p53, MDM2, and $p14^{ARF}$ as compared with other subtypes.

CONCLUSION: Elevated expression of p53, MDM2, and $p14^{ARF}$ in benign and malignant ameloblastomas suggests that alteration of the p53–MDM2–$p14^{ARF}$ cascade is involved in oncogenesis and/of malignant transformation of odontogenic epithelium. *p53* gene status implied that *p53* mutation might play a minor role in neoplastic changes of odontogenic epithelium. Immunoreactivity for p53, MDM2, and $p14^{ARF}$ in ameloblastoma variants suggests that these factors might be associated with tissue structuring and cytodifferentiation of ameloblastomas.

J Oral Pathol Med (2004) **33**: 292–9

Keywords: ameloblastoma; MDM2; $p14^{ARF}$; p53

Correspondence: Hiroyuki Kumamoto, Division of Oral Pathology, Department of Oral Medicine and Surgery, Tohoku University Graduate School of Dentistry, 4-1 Seiryo-machi, Aoba-ku, Sendai 980-8575, Japan. Tel.: +81 22 717 8303. Fax: +81 22 717 8304. E-mail: kumamoto@mail.tains.tohoku.ac.jp
Accepted for publication September 15, 2003

Introduction

Tumors arising from epithelium of the odontogenic apparatus or from its derivatives or remnants exhibit considerable histologic variation and are classified into several benign and malignant entities (1–4). Ameloblastoma is the most frequently encountered tumor arising from odontogenic epithelium and is characterized by a benign but locally invasive behavior with a high risk of recurrence (1, 2, 4). Histologically, ameloblastoma shows considerable variation, including follicular, plexiform, acanthomatous, granular cell, basal cell, and desmoplastic types (1). Malignant ameloblastoma is defined as a neoplasm in which the pattern of an ameloblastoma and cytologic features of malignancy are shown by the primary growth in the jaws and/or by any metastatic growth (1). Recently, malignant ameloblastoma has been subclassified into metastasizing ameloblastoma and ameloblastic carcinoma on the basis of metastatic spread and cytologic malignant features (3). Several recent studies have detected genetic and cytogenetic alterations in these epithelial odontogenic tumors (5–8); however, the detailed mechanisms of oncogenesis, cytodifferentiation, and tumor progression remain unknown.

A series of genetic alterations appears to promote the development of tumors via multiple steps (9, 10). *p53* gene is well recognized as a tumor suppressor gene situated on chromosome 17p13 and is one of the most frequently altered genes in tumors (11–13). Its gene product is a transcriptional factor that plays an important role in response to cellular DNA damage by inducing either G1/S cell cycle arrest to allow DNA repair or apoptosis if DNA has suffered irreversible damage (13, 14). Mutation and loss of heterozygosity

(LOH) of *p53* gene and/or accumulation of p53 product protein have been associated with increased cellular proliferation and malignant transformation (10, 12, 15–21). *MDM2* gene, mapped to chromosome 12q13-14, was originally identified as a highly amplified gene in a transformed tumorigenic fibroblast cell line (22). Its product protein forms a tight complex with both wild- and mutant-type p53 protein and inactivates wild-type p53 function (23). Amplification of *MDM2* gene and overexpression of its product protein have been reported to be involved in tumorigenesis or tumor development in several human malignancies (7, 17, 19, 24). $p14^{ARF}$ gene is located at the INK4a/ARF locus on chromosome 9p21, a region with a high rate of LOH in human tumors, and shared exons with $p16^{INK4a}$ gene, which encodes a cyclin-dependent kinase inhibitor, in an alternative reading frame (25, 26). $p14^{ARF}$ product directly interacts with MDM2 and neutralizes MDM2-mediated inhibition of p53 (27). Certain tumors have shown $p14^{ARF}$ gene alterations, including LOH, mutation, and hypermethylation (21, 28, 29).

Our previous studies confirmed cellular kinetics, including proliferation and cell death modulators, in tooth germs and ameloblastomas, suggesting that these factors are associated with oncogenesis or cytodifferentiation of odontogenic epithelium (26, 30–34). Several studies have examined alteration of *p53* gene and expression of p53 and MDM2 proteins in specific odontogenic tumors (7, 8, 18, 35). In the present study, the immunohistochemical expression of p53, MDM2, and $p14^{ARF}$ proteins and mutation of *p53* gene was examined in ameloblastomas as well as in tooth germs to clarify the possible role of p53 and its upstream regulators in epithelial odontogenic tumors.

Materials and methods

The study protocol was reviewed and approved by the Research Ethics Committee of Tohoku University Graduate School of Dentistry.

Tissue preparation

Specimens were surgically removed from 51 patients with epithelial odontogenic tumor at the Department of Oral and Maxillofacial Surgery, Tohoku University Dental Hospital, and affiliated hospitals. The specimens were fixed in 10% buffered formalin for one to several days and were embedded in paraffin. The tissue blocks were sliced into 3-μm thick sections for routine histologic and subsequent immunohistochemical examinations. Tissue sections were stained with hematoxylin and eosin for histologic diagnosis according to the WHO histologic typing of odontogenic tumors (1). The tumors comprised 46 ameloblastomas and 5 malignant ameloblastomas. Ameloblastomas were divided into 29 follicular and 17 plexiform types, including 17 acanthomatous, 5 granular cell, 3 basal cell, and 4 desmoplastic subtypes. Malignant ameloblastomas were classified into two metastasizing ameloblastomas and three ameloblastic carcinomas according to the criteria provided by Eversole (3). For direct DNA sequencing, tumor tissues were immediately frozen on dry ice and stored at −80°C. Specimens of 16 tooth germs of the mandibular third molars, enucleated for orthodontic reasons at the stage of crown mineralization, were similarly prepared and compared with the epithelial odontogenic tumors.

Immunohistochemistry for p53, MDM2, and $p14^{ARF}$ expression

The tissue sections were deparaffinized and immersed in methanol with 0.3% hydrogen peroxide. For antigen retrieval, the sections were heated in 0.01 M citrate buffer (pH 6.0) for 10 min by autoclave (121°C, 2 atm). After treatment with normal serum for 30 min, the sections were incubated with primary antibodies at 4°C overnight. The applied antibodies were mouse anti-p53 monoclonal antibody (Dako, Glostrup, Denmark; subclass IgG2b; diluted at 1 : 50), mouse anti-MDM2 monoclonal antibody (Santa Cruz Biotechnology, Santa Cruz, CA, USA; subclass IgG1; diluted at 1 : 200), and rabbit anti-$p14^{ARF}$ polyclonal antibody (Santa Cruz Biotechnology; diluted at 1 : 200). The standard streptavidin–biotin–peroxidase complex method was performed to bind the primary antibodies with the use of Histofine SAB-PO Kits (Nichirei, Tokyo, Japan). Reaction products were visualized by immersing the sections in 0.03% diaminobenzidine solution containing 2 mM hydrogen peroxide for 1–3 min. Nuclei were lightly counterstained with methylgreen. For control studies of the antibodies, the serial sections were treated with phosphate-buffered saline, mouse anti-chromogranin A monoclonal antibody (Dako; subclass IgG2b), mouse anti-desmin monoclonal antibody (Nichirei; subclass IgG1), and normal rabbit IgG instead of the primary antibodies and were confirmed to be unstained.

Immunohistochemical reactivity for p53, MDM2, and $p14^{ARF}$ was evaluated and classified into four groups: (−) negative, (±) weakly positive (less than 5% of epithelial or neoplastic cells), (+) moderately positive (5–25% of epithelial or neoplastic cells), and (++) strongly positive (more than 25% of epithelial or neoplastic cells) positive. The statistical significance of differences in the percentages of cases with different reactivity levels was analyzed by the Mann–Whitney *U*-test for differences between two groups or the Kruskal–Wallis test for differences among three or more groups. *P*-values less than 0.05 were considered to indicate statistical significance.

Direct DNA sequencing for p53 gene mutation

Genomic DNA was extracted from frozen tissue samples of 10 benign ameloblastomas and 1 malignant ameloblastoma, which immunohistochemically showed moderately positive (+) reactions for p53 protein, using a QIAamp DNA Mini

Table 1 Primers for *p53* sequencing

Exon	*Codon*	*Sequence (5′–3′)*	*Product (bp)*
5	146–186	Forward: GCTGTGGGTTGATTCCACAC	167
		Reverse: AACCAGCCCTGTCGTCTCTC	
6	187–224	Forward: GCCTCTGTTCCTCACTGATT	175
		Reverse: TCCTCCCAGAGACCCCAGTT	
7	225–261	Forward: CCTCATCTTGGGCCTGTGTT	171
		Reverse: CAGTGTGCAGGGTGGCAAGT	
8	262–306	Forward: TTCCTTACTGCCTCTTGCTT	206
		Reverse: CACCGCTTCTTGTCCTGCTT	

Kit (Qiagen, Hilden, Germany). *p53* exons 5–8, where most mutations of *p53* gene occur in human tumors, were separately amplified using a HotstarTaq Master Mix Kit (Qiagen) with specific primers (Table 1) in a DNA thermal cycler (Eppendorf, Hamburg, Germany). Polymerase chain reaction (PCR) was performed in a total volume of 50 µl, containing 0.5 µg of template DNA and 0.5 mM of each specific primer set. The procedure for amplification included 35 cycles of denaturation at 94°C for 45 s, annealing at 55°C for 45 s and elongation at 72°C for 60 s with heat starting at 95°C for 15 min and final elongation at 72°C for 10 min.

Sequencing reactions of each *p53* exon were carried out with the PCR products purified using a GFR PCR DNA and Gel Band Purification Kit (Amersham Biosciences, Little Chalfont, UK), the above-mentioned PCR primers and a Thermo Sequenase Cy5 Dye Terminator Sequencing Kit (Amersham Biosciences). The sequencing products were separated on denaturing 8% polyacrylamide gel on an automated laser fluorescence sequencer (ALFexpress II DNA Sequencer; Amersham Biosciences), and the sequencing data were analyzed with the use of an ALFwin Sequence Analyser (Amersham Biosciences).

Results

Immunohistochemical reactivity for p53, MDM2, and p14ARF

The results of immunohistochemical studies of p53, MDM2, and $p14^{ARF}$ are summarized in Table 2. Immunohistochemical reactivity for p53 was detected in the nuclei of normal and neoplastic odontogenic epithelial cells (Fig. 1). In tooth germs, p53 expression was found in limited epithelial cells in 2 of 13 dental laminae. Ameloblastomas showed p53 reactivity scatteredly in peripheral columnar or cuboidal cells in 13 of 29 follicular cases and 16 of 17 plexiform cases (Fig. 1A,B). p53 expression in ameloblastomas was significantly higher than that in enamel organs ($P < 0.05$) and dental laminae ($P < 0.01$) of tooth germs. Plexiform ameloblastomas exhibited statistically higher p53 expression than follicular ameloblastomas ($P < 0.001$). Keratinizing cells in acanthomatous ameloblastomas and granular cells in granular cell ameloblastomas were not reactive with anti-p53 antibody. Basal cell ameloblastomas showed p53 reactivity in scattered neoplastic cells, whereas p53 expression in desmoplastic ameloblastomas was found in a few neoplastic cells. Expression of p53 in malignant ameloblastomas was detected in all five cases and was significantly higher than that in enamel organs and dental laminae ($P < 0.01$). Metastasizing ameloblastomas showed a p53 expression pattern similar to that of follicular ameloblastomas, while ameloblastic carcinomas demonstrated increased p53 expression in neoplastic cells (Fig. 1C).

Immunohistochemical reactivity for MDM2 and $p14^{ARF}$ was detected in the nuclei of normal and neoplastic odontogenic epithelial cells: mesenchymal cells in tooth germs and stromal cells in benign and malignant ameloblastomas were faintly reactive with anti-MDM2 and anti-$p14^{ARF}$ antibodies (Figs. 2 and 3). In all tooth germs, MDM2 expression was found in scattered epithelial cells of outer enamel epithelium and dental laminae. Ameloblastomas showed MDM2 reactivity in many peripheral columnar or

Table 2 Immunohistochemical reactivity for p53, MDM2, and $p14^{ARF}$ proteins in tooth germs and ameloblastomas

	p53				*MDM2*				*p14ARF*			
	(–)	(±)	(+)	(++)	(–)	(±)	(+)	(++)	(–)	(±)	(+)	(++)
Tooth germ ($n = 16$)												
Enamel organ ($n = 8$)	8 (100)	0 (0)	0 (0)	0 (0)	0 (0)	2 (25)	6 (75)	0 (0)	2 (25)	5 (62)	1 (13)	0 (0)
Dental lamina ($n = 13$)	11 (85)	2 (15)	0 (0)	0 (0)	0 (0)	2 (15)	6 (47)	5 (38)	0 (0)	5 (38)	4 (31)	4 (31)
Ameloblastoma ($n = 46$)	17 (37)	9 (20)	20 (43)	0 (0)	0 (0)	3 (7)	17 (37)	26 (56)	0 (0)	5 (11)	30 (65)	11 (24)
Follicular type ($n = 29$)	16 (55)	6 (21)	7 (24)	0 (0)	0 (0)	3 (10)	14 (48)	12 (42)	0 (0)	4 (14)	23 (79)	2 (7)
Plexiform type ($n = 17$)	1 (6)	3 (18)	13 (76)	0 (0)	0 (0)	0 (0)	3 (18)	14 (82)	0 (0)	1 (6)	7 (41)	9 (53)
Acanthomatous subtype ($n = 17$)	6 (35)	2 (12)	9 (53)	0 (0)	0 (0)	2 (12)	7 (41)	8 (47)	0 (0)	2 (12)	13 (76)	2 (12)
Granular subtype ($n = 5$)	2 (40)	3 (60)	0 (0)	0 (0)	0 (0)	1 (20)	3 (60)	1 (20)	0 (0)	1 (20)	4 (80)	0 (0)
Basal cell subtype ($n = 3$)	0 (0)	0 (0)	3 (100)	0 (0)	0 (0)	0 (0)	1 (33)	2 (67)	0 (0)	0 (0)	0 (0)	3 (100)
Desmoplastic subtype ($n = 4$)	2 (50)	2 (50)	0 (0)	0 (0)	0 (0)	0 (0)	0 (0)	4 (100)	0 (0)	0 (0)	4 (100)	0 (0)
Malignant ameloblastoma ($n = 5$)	0 (0)	2 (40)	2 (40)	1 (20)	0 (0)	1 (20)	0 (0)	4 (80)	0 (0)	0 (0)	2 (40)	3 (60)
Metastasizing ameloblastoma ($n = 2$)	0 (0)	1 (50)	1 (50)	0 (0)	0 (0)	1 (50)	0 (0)	1 (50)	0 (0)	0 (0)	2 (100)	0 (0)
Ameloblastoma carcinoma ($n = 3$)	0 (0)	1 (33)	1 (33)	1 (33)	0 (0)	0 (0)	0 (0)	3 (100)	0 (0)	0 (0)	0 (0)	3 (0)

Immunohistochemical reactivity: (–) negative; (±) weakly (less than 5% of epithelial or neoplastic cells) positive; (+) moderately (5–25% of epithelial or neoplastic cells) positive; (++) strongly (more than 25% of epithelial or neoplastic cells) positive.
Values in parentheses denote percentage values.
Statistical significance: $^{*}P < 0.05$; $^{**}P < 0.01$; $^{***}P < 0.001$.

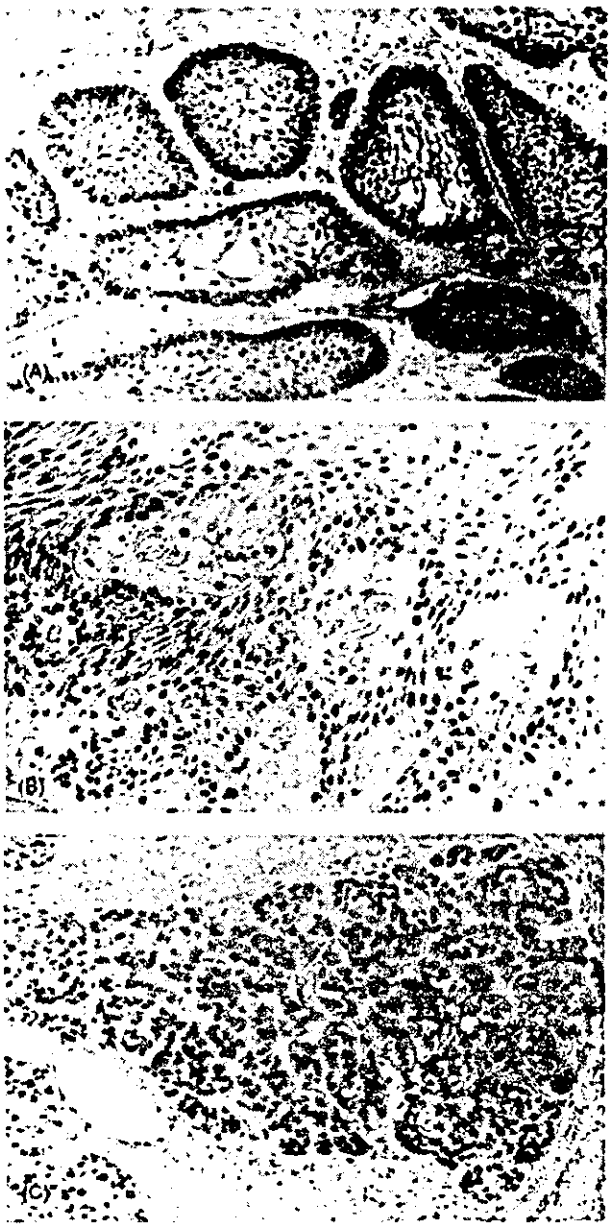

Figure 1 Immunohistochemical reactivity for p53 in ameloblastoma (A,B) and malignant ameloblastoma (C). Follicular ameloblastoma (A) and plexiform ameloblastoma (B) showing reactivity scatteredly in peripheral columnar or cuboidal cells (A: ×160; B: ×160). Ameloblastic carcinoma (C) showing reactivity in most neoplastic cells (×160).

Figure 2 Immunohistochemical reactivity for MDM2 in ameloblastoma (A,B) and malignant ameloblastoma (C). (A) Plexiform ameloblastoma showing reactivity in many peripheral cuboidal cells and some central polyhedral cells (×175). (B) Granular cell ameloblastoma showing a little reactivity in granular cells (×140). (C) Ameloblastic carcinoma showing reactivity in most neoplastic cells (×180).

cuboidal cells and some central polyhedral cells in all cases (Fig. 2A). MDM2 expression in ameloblastomas was significantly higher than that in enamel organs of tooth germs ($P < 0.05$). Plexiform ameloblastomas exhibited statistically higher MDM2 expression than follicular ameloblastomas ($P < 0.01$). MDM2 reactivity was markedly decreased in keratinizing cells in acanthomatous ameloblastomas and granular cells in granular cell ameloblastomas (Fig. 2B). Basal cell ameloblastomas and desmoplastic ameloblastomas showed diffuse MDM2 expression in neoplastic cells, and staining intensity in desmoplastic ameloblastomas was low. Expression of MDM2 in malignant ameloblastomas was detected in all cases. Metastasizing ameloblastomas showed a MDM2 expression pattern similar to that of follicular ameloblastomas, while ameloblastic carcinomas were diffusely positive for MDM2 in most neoplastic cells (Fig. 2C).

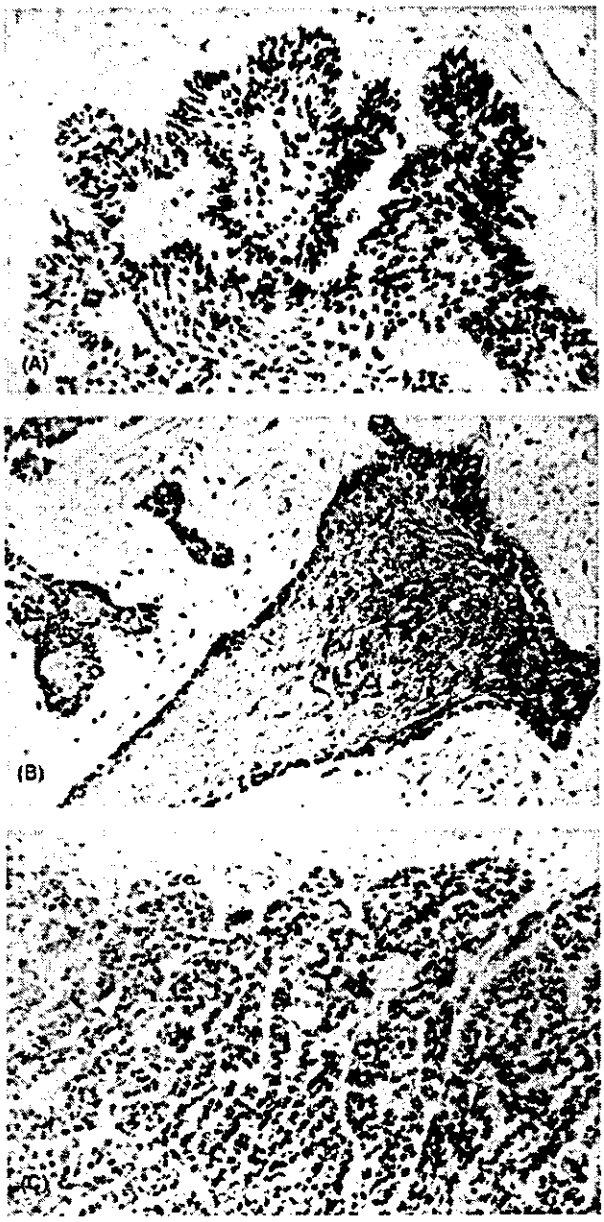

Figure 3 Immunohistochemical reactivity for p14^{ARF} in ameloblastoma (A,B) and malignant ameloblastoma (C). (A) Follicular ameloblastoma showing reactivity in many peripheral columnar cells and some central polyhedral cells (×160). (B) Desmoplastic ameloblastoma showing reactivity in neoplastic cells neighboring the basement membrane (×130). (C) Ameloblastic carcinoma showing reactivity in most neoplastic cells (×140).

p14^{ARF} expression was found in scattered epithelial cells of outer enamel epithelium and dental laminae in all but two tooth germs, and dental laminae showed significantly higher p14^{ARF} expression than enamel organs did ($P < 0.05$). Ameloblastomas showed p14^{ARF} reactivity in many peripheral columnar or cuboidal cells and some central polyhedral cells in all cases (Fig. 3A). p14^{ARF} expression in ameloblastomas was significantly higher than that in enamel organs of tooth germs ($P < 0.01$). Plexiform ameloblastomas exhibited statistically higher p14^{ARF} expression than follicular ameloblastomas ($P < 0.01$). Keratinizing cells in acanthomatous ameloblastomas and granular cells in granular cell ameloblastomas demonstrated little or no reactivity for p14^{ARF}. Basal cell ameloblastomas showed diffused p14^{ARF} expression in neoplastic cells, whereas p14^{ARF} reactivity in desmoplastic ameloblastomas was localized in neoplastic cells neighboring the basement membrane (Fig. 3B). p14^{ARF} expression in basal cell ameloblastomas was significantly higher than that in acanthomatous ameloblastomas ($P < 0.05$) and granular cell ameloblastomas ($P < 0.01$). Expression of p14^{ARF} in malignant ameloblastomas was detected in all cases and was significantly higher than that in enamel organs of tooth germs ($P < 0.01$). Metastasizing ameloblastomas showed a p14^{ARF} expression pattern similar to that of follicular ameloblastomas, while ameloblastic carcinomas were diffusely positive for p14^{ARF} in most neoplastic cells (Fig. 3C). Ameloblastic carcinomas exhibited statistically higher p14^{ARF} expression than metastasizing ameloblastomas ($P < 0.05$).

Mutation analysis of p53 gene

Direct DNA sequencing for *p53* gene mutation was carried out in 10 ameloblastomas (five follicular and five plexiform cases) and 1 malignant ameloblastoma (one metastasizing ameloblastoma), which were moderately positive for p53 protein. Mutational alteration was not detected in *p53* gene exons 5–8, including hotspot codons 175, 245, 248, 249, 273, and 282, in any of the 11 cases (Fig. 4).

Discussion

Mutation of *p53* gene results in accumulation of a conformationally altered and functionally defective protein, and overexpression of p53 protein has been detected in various types of tumors (17–21). The present study was performed, employing a monoclonal antibody reactive with wild- and mutant-type p53 protein. Tooth germ tissue showed no or little p53 expression, whereas nuclear accumulation was recognized in benign and malignant ameloblastomas. These features suggest that p53 expression is associated with oncogenesis of odontogenic epithelium. In ameloblastomas, reactivity for p53 was significantly higher in plexiform-type than in follicular-type, suggesting that tissue structuring of ameloblastomas might be affected by p53 expression. In our previous study, keratinizing cells in acanthomatous ameloblastomas and granular cells in granular cell ameloblastomas showed increased apoptotic cell death as compared with other neoplastic cells (30, 32). The present study found no p53 expression in keratinizing or granular cells in ameloblastomas. Apoptosis of these cells was thus apparently not induced by a p53-dependent pathway.

In a wide variety of human tumors, *p53* gene mutations have been detected mainly in exons 5–8, including several hotspot codons (10, 12, 13, 15, 16, 19, 21). Ameloblastomas have shown infrequent *p53* mutations in limited number of neoplastic cells on ELISA and yeast functional assay (7, 8). In the present study using direct *p53* sequencing, alteration of *p53* exons 5–8 was not detected in 10 benign ameloblastomas or 1 metastasizing ameloblastoma, although these

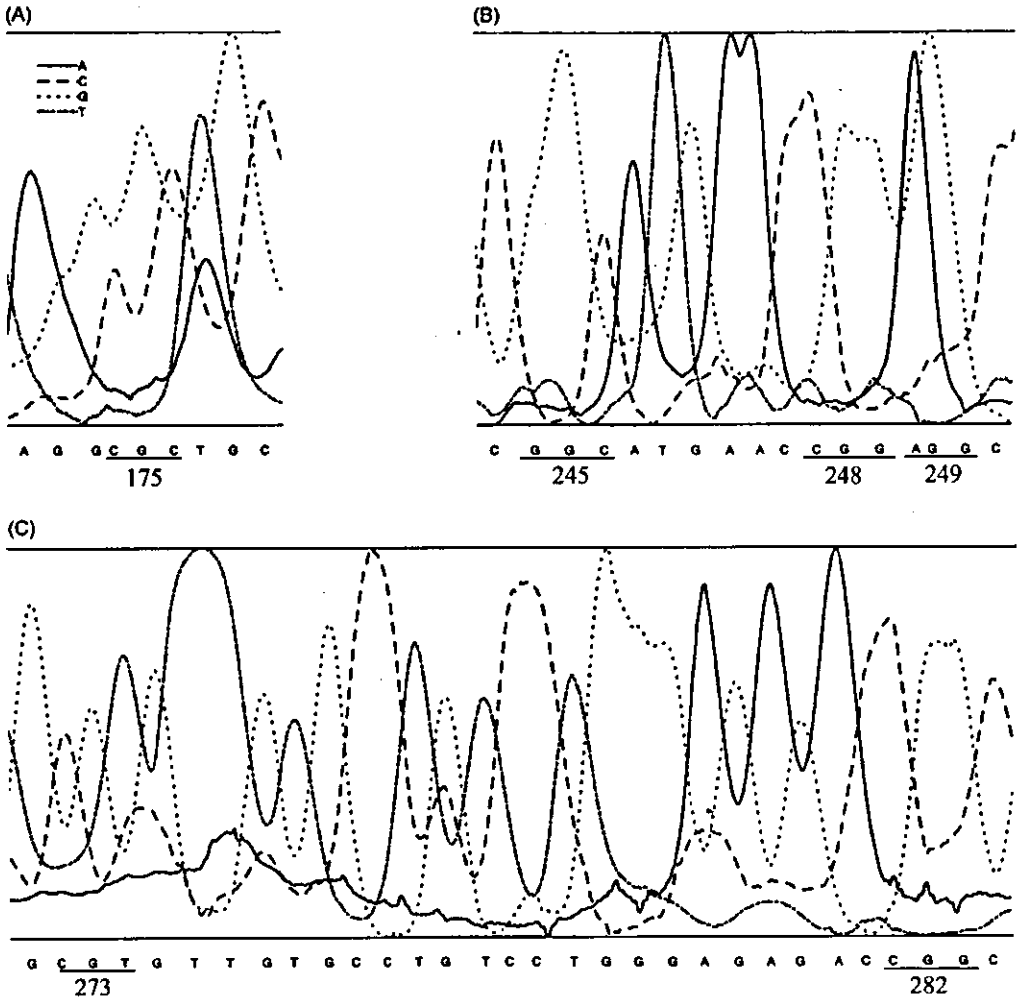

Figure 4 Direct DNA sequencing of *p53* gene in ameloblastoma. No mutation is detected at hotspot codons: codon 175 in exon 5 (A), codons 245, 248, and 249 in exon 7 (B) and codons 273 and 282 in exon 8 (C).

cases were immunohistochemically positive for p53. These findings suggest that mutation of *p53* gene might play a minor role in, and not be essential for, neoplastic changes of odontogenic epithelium. Wild-type p53 protein transcriptionally activates genes involved in cell cycle arrest, such as $p21^{WAF1/Cip1}$, or genes modulating apoptosis, such as bax (13, 36). Our previous study demonstrated low reactivity for bax protein and obvious $p21^{WAF1/Cip1}$ expression in ameloblastomas (26, 31). These features indicate that wild-type p53 protein regulates the cell cycle via $p21^{WAF1/Cip1}$ protein in ameloblastomas. In the present study, several amcloblastic carcinomas immunohistochemically showed increased p53 reactivity, and p53 was possibly associated with malignant transformation of odontogenic epithelium. Mutation analysis of *p53* gene in ameloblastic carcinomas could not be investigated because of the rarity of the malignancy, and further studies should be carried out to determine the association between p53 and malignant changes of odontogenic epithelium. Kropveld et al. (37) has revealed that 33% of all mutations are located outside the core domain of *p53* gene in head and neck squamous cell carcinomas. In our study, mutation analysis was performed only in the core domain of *p53* gene, and sequencing analysis of all 11 exons might be needed to guarantee absence of *p53* mutations.

The $p14^{ARF}$–MDM2–p53 cascade, called the p53 pathway, is an important cell cycle regulatory system in G1 arrest (25, 38), and aberration of this system strongly correlates with neoplastic transformation (7, 17, 19, 21, 24, 28, 29). The ability to generate mice lacking *p53* implies that *p53* is dispensable for embryonic development, while expression of MDM2 and $p14^{ARF}$ during development suggests that these molecules have a primary role in developmental processes (13,39). In the present study, tooth germs showed higher immunohistochemical reactivity for MDM2 and $p14^{ARF}$ as compared with that for p53, indicating that MDM2 and $p14^{ARF}$ play certain roles in tooth development. MDM2 expression in ameloblastomas has been reported to be associated with proliferative activity (7). Our previous study revealed that expression of $p16^{INK4a}$ protein did not

differ distinctly between tooth germs and ameloblastomas (26). In the present study, expression of MDM2 and p14^{ARF} was higher in ameloblastomas and malignant ameloblastomas than in tooth germs, suggesting that these upstream regulators of p53 are involved in oncogenesis and/or malignant transformation of odontogenic epithelium. Plexiform ameloblastomas showed higher expression of MDM2 and p14^{ARF} than follicular ameloblastomas, and markedly decreased reactivity for MDM2 and p14^{ARF} was found in keratinizing and granular cells in ameloblastomas, similar to p53 expression in ameloblastomas. In addition, basal cell ameloblastomas demonstrated high reactivity for p53, MDM2, and p14^{ARF} as compared with other subtypes of ameloblastomas, and p14^{ARF} expression in desmoplastic ameloblastomas was localized in neoplastic cells of basal areas. These features suggest that the p53–MDM2–p14^{ARF} cell cycle regulation system might be related to tissue structuring and cytodifferentiation of ameloblastomas.

References

1. Kramer IRH, Pindborg JJ, Shear M. *WHO Histological Typing of Odontogenic Tumours*. Berlin: Springer-Verlag, 1992; 11–27.
2. Melrose RJ. Benign epithelial odontogenic tumors. *Semin Diagn Pathol* 1999; **16**: 271–87.
3. Eversole LR. Malignant epithelial odontogenic tumors. *Semin Diagn Pathol* 1999; **16**: 317–24.
4. Sciubba JJ, Fantasia JE, Kahn LB. *Tumors and Cysts of the Jaw*. Washington, DC: Armed Forces institute of Pathology, 2001; 71–99.
5. Heikinheimo K, Jee KJ, Niini T, et al. Gene expression profiling of ameloblastoma and human tooth germ by means of a cDNA microarray. *J Dent Res* 2002; **81**: 525–30.
6. Jaakelainen K, Jee KJ, Leivo I, Saloniemi I, Knuutila S, Heikinheimo K. Cell proliferation and chromosomal changes in human ameloblastoma. *Cancer Genet Cytogenet* 2002; **136**: 31–7.
7. Sandra F, Nakamura N, Kanematsu T, Hiarata M, Ohishi M. The role of MDM2 in the proliferative activity of ameloblastoma. *Oral Oncol* 2002; **38**: 163–7.
8. Shibata T, Nakata D, Chiba I, et al. Detection of TP53 mutation in ameloblastoma by the use of a yeast functional assay. *J Oral Pathol Med* 2002; **31**: 534–8.
9. Vogelstein B, Fearon ER, Hamilton SR, et al. Genetic alterations during colorectal-tumor development. *N Engl J Med* 1988; **319**: 525–32.
10. Yanoshita-Kikuchi R, Konishi M, Ito S, et al. Genetic changes of both p53 alleles associated with the conversion from colorectal adenoma to early carcinoma in familial adenomatous polyposis and non-familial adenomatous polyposis patients. *Cancer Res* 1992; **52**: 3965–71.
11. Finlay CA, Hinds PW, Levine AJ. The p53 proto-oncogene can act as a suppressor of transformation. *Cell* 1989; **57**: 1083–93.
12. Nigro JM, Baker SJ, Preisinger AC, et al. Mutations in the *p53* gene occur in diverse human tumour types. *Nature* 1989; **342**: 705–8.
13. Ko LJ, Prives C. p53: puzzle and paradigm. *Genes Dev* 1996; **10**: 1054–72.
14. Lane DP. p53, guardian of the genome. *Nature* 1992; **358**: 15–6.
15. Suzuki H, Takahashi T, Kuroishi T, et al. *p53* mutations in non-small cell lung cancer in Japan: association between mutations and smoking. *Cancer Res* 1992; **52**: 734–6.
16. Yokozaki H, Kuniyasu H, Kitadai Y, et al. p53 point mutations in primary gastric carcinomas. *J Cancer Res Clin Oncol* 1992; **119**: 67–70.
17. Lianes P, Orlow I, Zhang Z-F, et al. Altered patterns of MDM2 and TP53 expression in human bladder cancer. *J Natl Cancer Inst* 1994; **86**: 1325–30.
18. Slootweg PJ. p53 protein and Ki-67 reactivity in epithelial odontogenic lesions: an immunohistochemical study. *J Oral Pathol Med* 1995; **24**: 393–7.
19. Veloso M, Wrba F, Kaserer K, et al. *p53* gene status and expression of p53, mdm2, and p21Waf1/Cip1 proteins in colorectal cancer. *Virchows Arch* 2000; **437**: 241–7.
20. Ohki K, Kumamoto H, Ichinohasama R, et al. Genetic analysis of DNA microsatellite loci in salivary gland tumours: comparison with immunohistochemical detection of hMSH2 and p53 proteins. *Int J Oral Maxillofac Surg* 2001; **30**: 538–44.
21. Weber A, Bellmann U, Bootz F, Wittekind C, Tannapfel A. INK4a-ARF alterations and p53 mutations in primary and consecutive squamous cell carcinoma of the head and neck. *Virchows Arch* 2002; **441**: 133–42.
22. Cahilly-Snyder L, Yang-Feng T, Francke U, George DL. Molecular analysis and chromosomal mapping of amplified genes isolated form a transformed mouse 3T3 cell line. *Somat Cell Mol Genet* 1987; **13**: 235–44.
23. Momand J, Zambetti GP, Olson DC, George D, Levine AJ. The *mdm*-2 oncogene product forms a complex with the p53 protein and inhibits p53-mediated transactivation. *Cell* 1992; **69**: 1237–45.
24. Marchetti A, Buttitta F, Girlando S, et al. *mdm2* gene alterations and mdm2 protein expression in breast carcinomas. *J Pathol* 1995; **175**: 31–8.
25. Quelle DE, Zindy F, Ashmun RA, Sherr CJ. Alternative reading frames of the INK4a tumor suppressor gene encode two unrelated proteins capable of inducing cell cycle arrest. *Cell* 1995; **83**: 993–1000.
26. Kumamoto H, Kimi K, Ooya K. Detection of cell cycle-related factors in ameloblastomas. *J Oral Pathol Med* 2001; **30**: 309–15.
27. Pomerantz J, Schreiber-Agus N, Liégeois NJ, et al. The *Ink4a* tumor suppressor gene product, p19^{ARF}, interacts with MDM2 and neutralizes MDM2's inhibition of p53. *Cell* 1998; **92**: 713–23.
28. Gazzeri S, Valle VD, Chaussade L, Brambilla C, Larsen C-J, Brambilla E. The human p19^{ARF} protein encoded by the β transcript of the *p16^{INK4a}* gene is frequently lost in small call lung cancer. *Cancer Res* 1998; **58**: 3926–31.
29. Sato F, Harpaz N, Shibata D, et al. Hypermethylation of the *p14^{ARF}* gene in ulcerative colitis-associated colorectal carcinogenesis. *Cancer Res* 2002; **62**: 1148–51.
30. Kumamoto H. Detection of apoptosis-related factors and apoptotic cells in ameloblastomas: analysis by immunohistochemistry and an *in situ* DNA nick end-labelling method. *J Oral Pathol Med* 1997; **26**: 419–25.
31. Kumamoto H, Ooya K. Immunohistochemical analysis of bcl-2 family proteins in benign and malignant ameloblastomas. *J Oral Pathol Med* 1999; **28**: 343–9.
32. Kumamoto H, Kimi K, Ooya K. Immunohistochemical analysis of apoptosis-related factors (Fas, Fas ligand, caspase-3 and single-stranded DNA) in ameloblastomas. *J Oral Pathol Med* 2001; **30**: 596–602.
33. Kumamoto H, Kinouchi Y, Ooya K. Telomerase activity and telomerase reverse transcriptase (TERT) expression in ameloblastomas. *J Oral Pathol Med* 2001; **30**: 231–6.
34. Kumamoto H, Yoshida M, Ooya K. Immunohistochemical detection of hepatocyte growth factor, transforming growth factor-β and their receptors in epithelial odontogenic tumors. *J Oral Pathol Med* 2002; **31**: 539–48.

35. Carvalhais JN, de Aguiar MCF, de Araújo VC, de Araújo NS, Gomez RS. p53 and MDM2 expression in odontogenic cysts and tumours. *Oral Dis* 1999; **5**: 218–22.
36. El-Deiry WA, Tokino T, Velculescu VE, et al. WAF1, a potential mediator of p53 tumor suppression. *Cell* 1993; **75**: 817–25.
37. Kropveld A, Rozemuller EH, Leppers FG et al. Sequencing analysis of RNA and DNA of exons 1 through 11 shows p53 gene alterations to be present in almost 100% of head and neck squamous cell cancers. *Laboratory Invest* 1999; **79**: 347–53.
38. Sherr CJ. Tumor surveillance via the ARF-p53 pathway. *Genes Dev* 1998; **12**: 2984–91.
39. Zindy F, Quelle DE, Roussel MF, Sherr CJ. Expression of the p16^{INK4a} tumor suppressor versus other INK4 family members during mouse development and aging. *Oncogene* 1997; **15**: 203–11.

J Oral Pathol Med (2004) 33: 360–7

www.blackwellmunksgaard.com/jopm

K-*Ras* gene status and expression of Ras/mitogen-activated protein kinase (MAPK) signaling molecules in ameloblastomas

Hiroyuki Kumamoto[1], Nobuhiro Takahashi[2], Kiyoshi Ooya[1]

[1]*Division of Oral Pathology, Department of Oral Medicine and Surgery, and* [2]*Division of Oral Ecology and Biochemistry, Department of Oral Biology, Tohoku University Graduate School of Dentistry, Sendai, Japan*

BACKGROUND: To clarify the roles of rat sarcoma (Ras)/mitogen-activated protein kinase (MAPK) signaling pathway in oncogenesis and cytodifferentiation of odontogenic tumors, K-*Ras* gene status and expression of Ras, Raf1, MAPK/extracellular signal-regulated kinase (ERK) kinase (MEK)1, and ERK1/2 proteins were analyzed in ameloblastomas as well as in tooth germs.

METHODS: Paraffin sections of 10 tooth germs and 46 benign and 6 malignant ameloblastomas were examined immunohistochemically for the expression of K-Ras, Raf1, MEK1, and ERK1/2. Frozen tissue samples of 22 benign ameloblastomas and 1 malignant (metastasizing) ameloblastoma were analyzed by direct DNA sequencing to detect K-*Ras* gene alteration.

RESULTS: Immunohistochemical reactivity for K-Ras, Raf1, MEK1, and ERK1/2 was detected in both normal and neoplastic odontogenic epithelium, and these molecules were reactive chiefly with odontogenic epithelial cells neighboring the basement membrane. Plexiform ameloblastomas showed slightly stronger expression of these Ras/MAPK signaling molecules than follicular ameloblastomas. Keratinizing cells and granular cells showed decreased reactivity for the signaling molecules. Basal cell ameloblastomas showed slightly stronger reactivity for the signaling molecules than did the other subtypes. K-Ras immunoreactivity in malignant ameloblastomas was lower than that in dental lamina of tooth germs. Direct DNA sequencing showed a GGT to GCT point mutation at codon 12 of K-*Ras* gene in one ameloblastoma.

CONCLUSION: Expression of K-Ras, Raf1, MEK1, and ERK1/2 in tooth germs and ameloblastomas suggests that Ras/MAPK signaling pathway functions to regulate cell proliferation and differentiation in both normal and neoplastic odontogenic epithelium. K-*Ras* gene status implied that K-*Ras* mutations might play a minor role in oncogenesis of odontogenic epithelium.

J Oral Pathol Med (2004) **33**: 360–7

Keywords: ameloblastoma; ERK; K-Ras; MEK; Raf

Introduction

Tumors arising from epithelium of the odontogenic apparatus or from its derivatives or remnants exhibit considerable histologic variation and are classified into several benign and malignant entities (1–4). Ameloblastoma is the most frequently encountered tumor arising from odontogenic epithelium and is characterized by a benign but locally invasive behavior with a high risk of recurrence (1, 2, 4). Histologically, ameloblastoma shows considerable variation, including follicular, plexiform, acanthomatous, granular cell, basal cell, and desmoplastic types (1). Malignant ameloblastoma is defined as a neoplasm in which the pattern of an ameloblastoma and cytological features of malignancy are shown by the primary growth in the jaws and/or by any metastatic growth (1). Recently, malignant ameloblastoma has been subclassified into metastasizing ameloblastoma and ameloblastic carcinoma on the basis of metastatic spread and cytological malignant features (3). Several recent studies have detected genetic and cytogenetic alterations in these epithelial odontogenic tumors (5–7); however, the detailed mechanisms of oncogenesis, cytodifferentiation, and tumor progression remain unknown.

Ras proto-oncogenes were originally characterized on the basis of homology with the transforming genes of rat sarcoma viruses (v-*Ras*), and three *Ras* genes, H-*Ras*, K-*Ras*, and N-*Ras*, were identified in the mammalian genome (8–10). Activation of *Ras* genes by mutation contributes to malignant transformation, and K-*Ras* mutations have been detected in various human neoplasms (10–16). *Ras* genes encode highly similar

Correspondence: Hiroyuki Kumamoto, Division of Oral Pathology, Department of Oral Medicine and Surgery, Tohoku University Graduate School of Dentistry, 4-1 Seiryo-machi, Aoba-ku, Sendai 980-8575, Japan. Tel.: +81 227178303. Fax: +81 22 7178304. E-mail: kumamoto@mail.tains.tohoku.ac.jp
Accepted for publication October 21, 2003

guanine nucleotide-binding proteins of approximately 21 kDa ($p21^{Ras}$), and $p21^{Ras}$ is involved in the transduction of external stimuli most likely induced by growth factors (10, 17, 18). These stimuli activate $p21^{Ras}$ by inducing the exchange of GDP to GTP, and GTP-bound $p21^{Ras}$ contributes the activation of three closely related Raf serine/threonine kinases: Raf1, B-Raf, and A-Raf (10, 16, 18). In downstream, activated Raf phosphorylates and activates mitogen-activated protein kinase (MAPK) kinases, MAPK/extracellular signal-regulated kinase (ERK) kinase (MEK)1 and MEK2 (16,18). Phosphorylated MEK functions as dual-specificity kinases and phosphorylates tandem threonine and tyrosine residues in MAPK, ERK1, and ERK12 to activate them (16, 18). Once activated, ERK translocates to the nucleus and activates a variety of substrates, including nuclear transcription factors (16–18). Thus, Ras/MAPK signaling pathway functions as a key regulator of cell proliferation and differentiation, and aberration of involved signaling components has been identified in a various of human tumors (16, 18–23).

Our previous studies confirmed cellular kinetics, including proliferation and cell death modulators, in tooth germs and ameloblastomas, suggesting that these factors are associated with oncogenesis or cytodifferentiation of odontogenic epithelium (24–29). Several studies have examined the expression of specific Ras/MAPK signaling molecules in tooth germs or odontogenic cysts and tumors (30–32). In the present study, the immunohistochemical expression of K-Ras, Raf1, MEK1, and ERK1/2 proteins and mutation of K-*Ras* gene were examined in ameloblastomas as well as in tooth germs to clarify the possible role of Ras/MAPK signaling pathway in epithelial odontogenic tumors.

Materials and methods

The study protocol was reviewed and approved by the Research Ethics Committee of Tohoku University Graduate School of Dentistry.

Tissue preparation

Specimens were surgically removed from 52 patients with epithelial odontogenic tumors at the Department of Oral and Maxillofacial Surgery, Tohoku University Dental Hospital, and affiliated hospitals. The specimens were fixed in 10% buffered formalin for one to several days and embedded in paraffin. The tissue blocks were sliced into 3-μm-thick sections for routine histologic and subsequent immunohistochemical examinations. Tissue sections were stained with hematoxylin and eosin for histologic diagnosis according to the WHO histologic typing of odontogenic tumors (1). The tumors comprised 46 ameloblastomas and 6 malignant ameloblastomas. Ameloblastomas were divided into 30 follicular and 16 plexiform types, including 15 acanthomatous, 5 granular cell, 3 basal cell and 4 desmoplastic subtypes. Malignant ameloblastomas were classified into two metastasizing ameloblastomas and four ameloblastic carcinomas according to the criteria of Eversole (3). For direct DNA sequencing, tumor tissues were immediately frozen on dry ice and stored at −80°C. Specimens of 10 tooth germs of the mandibular third molars, enucleated for orthodontic reasons at the initial stage of crown mineralization, were similarly prepared and compared with the epithelial odontogenic tumors.

Immunohistochemistry for K-Ras, Raf1, MEK1, and ERK1/2 expression

The tissue sections were deparaffinized, immersed in methanol with 0.3% hydrogen peroxide, and heated in 0.01 M citrate buffer (pH 6.0) for 10 min by autoclave (121°C, 2 atm). After treatment with normal serum for 30 min, the sections were incubated with primary antibodies at 4°C overnight. The applied antibodies were mouse anti-K-Ras monoclonal antibody (Oncogene, Boston, MA, USA; subclass IgG2a; diluted at 1 : 20), mouse anti-Raf1 monoclonal antibody (Santa Cruz Biotechnology, Santa Cruz, CA, USA; subclass IgG1; diluted at 1 : 100), mouse anti-MEK1 monoclonal antibody (Santa Cruz Biotechnology; subclass IgG2b; diluted at 1 : 100), and rabbit anti-ERK1/2 polyclonal antibody (Cell Signaling Technology, Beverly, MA, USA; diluted at 1 : 20). The standard streptavidin-biotin-peroxidase complex method was performed to bind the primary antibodies with the use of Histofine SAB-PO Kits (Nichirei, Tokyo, Japan). Reaction products were visualized by immersing the sections in 0.03% diaminobenzidine solution containing 2 mM hydrogen peroxide for 1–3 min. Nuclei were lightly counterstained with methylgreen. For control studies of the antibodies, the serial sections were treated with phosphate-buffered saline, mouse anti-L26 (CD20) monoclonal antibody (Nichirei; subclass IgG2a), mouse anti-OPD4 (CD45RO) monoclonal antibody (Dako, Glostrup, Denmark; subclass IgG1), mouse antichromogranin A monoclonal antibody (Dako; subclass IgG2b), and normal rabbit IgG instead of the primary antibodies and were confirmed to be unstained.

Immunohistochemical reactivity for K-Ras, Raf1, MEK1, and ERK1/2 was evaluated and classified into three groups: (+) focally weak to moderate reactivity; (++) focally strong reactivity or diffusely weak to moderate reactivity; and (+++) diffusely strong reactivity. The statistical significance of differences in the percentages of cases with different reactivity levels was analyzed by the Mann–Whitney *U*-test for differences between two groups or the Kruskal–Wallis test for differences among three or more groups. *P*-values less than 0.05 were considered to indicate statistical significance.

Direct DNA sequencing for K-Ras gene mutations

Genomic DNA was extracted from frozen tissue samples of 22 benign ameloblastomas and 1 malignant ameloblastoma using a QIAamp DNA Mini Kit (Qiagen, Hilden, Germany). K-*Ras* exons 1 and 2, including hotspot codons 12, 13, and 61, were separately amplified using a HotstarTaq Master Mix Kit (Qiagen) with specific primers in a DNA thermal cycler (Eppendorf, Hamburg, Germany). Primers used in this study were as follows: 5′-GACTGAATATAAACTTGTGG-3′

(forward) and 5′-CTATTGTTGGATCATATTCG-3′ (reverse) for exon 1, yielding a 107-bp product, and 5′-GATTCCTACAGGAAGCAAGT-3′ (forward) and 5′-CTATAATGGTGAATATCTTTC-3′ (reverse) for exon 2, yielding a 185-bp product. Polymerase chain reaction (PCR) was performed in a total volume of 50 μl, containing 0.5 μg of template DNA, 1.5 mM (for exon 1) or 3 mM (for exon 2) of $MgCl_2$, and 0.5 mM of each specific primer set. The procedure for amplification included 35 cycles of denaturation at 94°C for 45 s, annealing at 55°C for 45 s, and elongation at 72°C for 60 s, with heat starting at 95°C for 15 min, and final elongation at 72°C for 10 min.

Sequencing reactions of each K-*Ras* exon were carried out with the PCR products purified using an GFR PCR DNA and Gel Band Purification Kit (Amersham Biosciences, Little Chalfont, UK), the above-mentioned PCR primers, and a Thermo Sequenase Cy5 Dye Terminator Sequencing Kit (Amersham Biosciences). The sequencing products were separated on denatured 8% polyacrylamide gel on an automated laser fluorescence sequencer (ALFexpress II DNA Sequencer; Amersham Biosciences), and the sequencing data were analyzed with the use of an ALFwin Sequence Analyzer (Amersham Biosciences).

Results

Immunohistochemical reactivity for K-Ras, Raf1, MEK1, and ERK1/2

Immunohistochemical reactivity for K-Ras was detected in the cytoplasm and cell membrane of normal and neoplastic odontogenic epithelial cells (Fig. 1). In tooth germs, K-Ras reactivity in inner and outer enamel epithelium and dental lamina was more evident than that in stratum intermedium and stellate reticulum (Fig. 1A). Ameloblastomas showed K-Ras reactivity in many peripheral columnar or cuboidal cells and some central polyhedral cells (Fig. 1B). K-Ras expression in keratinizing cells in acanthomatous ameloblastomas and granular cells in granular cell ameloblastomas was low. Basal cell ameloblastomas and desmoplastic ameloblastomas showed K-Ras reactivity in most neoplastic cells. Metastasizing ameloblastomas showed a K-Ras expression pattern similar to that of follicular ameloblastomas, while ameloblastic carcinomas demonstrated weak to moderate K-Ras reactivity in neoplastic cells (Fig. 1C). Reactivity for K-Ras in malignant ameloblastomas was significantly lower than that in dental lamina ($P < 0.05$) (Table 1).

Expression of Raf1 and MEK1 was found in the cytoplasm of normal and neoplastic odontogenic epithelial cells (Figs. 2 and 3). Tooth germs showed Raf reactivity in inner enamel epithelium and dental lamina (Fig. 2A). In ameloblastomas, Raf1 reactivity in peripheral columnar or cuboidal cells was more evident than that in central polyhedral cells. Plexiform ameloblastomas exhibited statistically higher Raf1 expression than follicular ameloblastomas ($P < 0.05$) (Table 1). Keratinizing cells in acanthomatous ameloblastomas and granular cells in granular cell ameloblastomas showed markedly decreased reactivity for Raf1. Basal cell ameloblastomas and desmoplastic ameloblastomas showed diffuse Raf1 expression in neoplastic cells, and staining intensity in basal cell ameloblastomas was

Figure 1 Immunohistochemical reactivity for K-Ras. (A) Tooth germ showing moderate to strong reactivity in inner and outer enamel epithelium and weak reactivity in stratum intermedium and stellate reticulum (×100). (B) Follicular ameloblastoma showing strong reactivity in peripheral columnar cells and weak to moderate reactivity in central polyhedral cells (×125). (C) Ameloblastic carcinoma showing weak reactivity in most neoplastic cells (×120).

Table 1 Immunohistochemical reactivity for K-Ras, Raf1, MEK1, and ERK1/2 in tooth germs and ameloblastomas

	K-Ras			*Raf1*			*MEK1*			*ERK1/2*		
	(+)	(++)	(+++)	(+)	(++)	(+++)	(+)	(++)	(+++)	(+)	(++)	(+++)
Tooth germ (n = 10)												
Enamel organ (n = 10)	0 (0%)	7 (70%)	3 (30%)	0 (0%)	10 (100%)	0 (0%)	0 (0%)	6 (60%)	4 (40%)	0 (0%)	5 (50%)	5 (50%)
Dental lamina (n = 5)	0 (0%)	3 (60%)	2 (40%)	0 (0%)	5 (100%)	0 (0%)	0 (0%)	2 (40%)	3 (60%)	0 (0%)	2 (40%)	3 (60%)
Ameloblastoma (n = 46)	4 (9%)	38 (82%)	4 (9%)	5 (11%)	30 (65%)	11 (24%)	1 (2%)	32 (70%)	13 (28%)	4 (9%)	29 (63%)	13 (28%)
Follicular type (n = 30)	4 (13%)	24 (80%)	2 (7%)	4 (13%)	22 (74%)	4 (13%)	1 (3%)	20 (67%)	9 (30%)	4 (13%)	19 (64%)	7 (23%)
Plexiform type (n = 16)	0 (0%)	14 (87%)	2 (13%)	1 (6%)	8 (50%)	7 (44%)	0 (0%)	12 (75%)	4 (25%)	0 (0%)	10 (62%)	6 (38%)
Acanthomatous subtype (n = 15)	2 (13%)	11 (74%)	2 (13%)	3 (20%)	10 (67%)	2 (13%)	0 (0%)	12 (80%)	3 (20%)	1 (9%)	10 (66%)	4 (27%)
Granular subtype (n = 5)	1 (20%)	4 (80%)	0 (0%)	1 (20%)	3 (60%)	1 (20%)	0 (0%)	4 (80%)	1 (20%)	1 (20%)	4 (80%)	0 (0%)
Basal cell subtype (n = 3)	0 (0%)	2 (67%)	1 (33%)	0 (0%)	1 (33%)	2 (67%)	0 (0%)	2 (67%)	1 (33%)	0 (0%)	1 (33%)	2 (67%)
Desmoplastic subtype (n = 4)	0 (0%)	4 (100%)	0 (0%)	0 (0 %)	4 (100%)	0 (0%)	0 (0%)	3 (75%)	1 (25%)	0 (0%)	1 (25%)	3 (75%)
Malignant ameloblastoma (n = 6)	1 (17%)	5 (83%)	0 (0%)	1 (17%)	4 (66%)	1 (17%)	0 (0%)	4 (67%)	2 (33%)	0 (0%)	4 (67%)	2 (33%)
Metastasizing ameloblastoma (n = 2)	0 (0%)	2 (100%)	0 (0%)	0 (0%)	2 (100%)	0 (0%)	0 (0%)	2 (100%)	0 (0%)	0 (0%)	2 (100%)	0 (0%)
Ameloblastic carcinoma (n = 4)	1 (25%)	3 (75%)	0 (0%)	1 (25%)	2 (50%)	1 (25%)	0 (0%)	2 (50%)	2 (50%)	0 (0%)	2 (50%)	2 (50%)

Immunohistochemical reactivity: (+) focally weak to moderate reactivity; (++) focally strong reactivity or diffusely weak to moderate reactivity; (+++) diffusely strong reactivity.
Statistical significance: * $P < 0.05$.

Figure 2 Immunohistochemical reactivity for Raf1. (A) Tooth germ showing reactivity in inner enamel epithelium (×105). (B) Basal cell ameloblastoma showing reactivity in most neoplastic cells (×115). (C) Ameloblastic carcinoma showing reactivity in most neoplastic cells (×115).

remarkable (Fig. 2B). Metastasizing ameloblastomas showed a Raf1 expression pattern similar to that of follicular ameloblastomas, while ameloblastic carcinomas were positive for Raf1 in most neoplastic cells (Fig. 2C).

Figure 3 Immunohistochemical reactivity for MEK1. (A) Tooth germ showing strong reactivity in inner enamel epithelium and weak to moderate reactivity in outer enamel epithelium, stratum intermedium and stellate reticulum (×100). (B) Plexiform ameloblastoma showing strong reactivity in peripheral columnar or cuboidal cells and weak to moderate reactivity in central polyhedral cells (×125). (C) Ameloblastic carcinoma showing strong reactivity in most neoplastic cells (×100).

MEK1 expression was detected in most epithelial cells in tooth germs, and reactivity in inner enamel epithelium was stronger than that in other epithelial components (Fig. 3A). Ameloblastomas showed MEK1 expression in most neoplastic cells, and reactivity in peripheral columnar or cuboidal calls was stronger than that in central polyhedral cells (Fig. 3B). Keratinizing cells in acanthomatous ameloblastomas and granular cells in granular cell ameloblastomas demonstrated low reactivity for MEK1. Basal cell ameloblastomas and desmoplastic ameloblastomas showed diffuse MEK1 expression in neoplastic cells. Metastasizing ameloblastomas showed a MEK1 expression pattern similar to that of follicular ameloblastomas, while ameloblastic carcinomas were moderately to strongly positive for MEK1 in most neoplastic cells (Fig. 3C).

Immunohistochemical reactivity for ERK1/2 was detected usually in the cytoplasm and often in the nuclei of normal and neoplastic odontogenic epithelial cells (Fig. 4). In tooth germs, ERK1/2 expression was found in most epithelial cells, and reactivity in inner and outer enamel epithelium was stronger than that in other epithelial components (Fig. 4A). Ameloblastomas showed ERK1/2 expression in most neoplastic cells, and reactivity in peripheral columnar or cuboidal cells was stronger than that in central polyhedral cells. Keratinizing cells in acanthomatous ameloblastomas and granular cells in granular cell ameloblastomas demonstrated markedly decreased reactivity for ERK1/2 (Fig. 4B). Basal cell ameloblastomas and desmoplastic ameloblastomas showed diffuse ERK1/2 expression in neoplastic cells. Metastasizing ameloblastomas showed a ERK1/2 expression pattern similar to that of follicular ameloblastomas, while ameloblastic carcinomas were moderately to strongly positive for ERK1/2 in most neoplastic cells (Fig. 4C).

*Mutation analysis of K-*Ras *gene*

Direct DNA sequencing for K-*Ras* gene mutations was carried out in 22 ameloblastomas (13 follicular and 9 plexiform cases, including 7 acanthomatous, 3 granular cell, 1 basal cell and 1 desmoplastic subtypes) and 1 malignant ameloblastoma (1 metastasizing ameloblastoma). A GGT to GCT (glycine to alanine) point mutation was detected at codon 12 in exon 1 of K-*Ras* gene in one follicular ameloblastoma without cellular subtype (Fig. 5). Mutational alteration was not detected at codon 13 in exon 1 or codon 61 in exon 2 of K-*Ras* gene in any of the 23 cases.

Discussion

RAS/MAPK signaling pathway is a primordial signaling system that controls such fundamental cellular processes as cell proliferation and differentiation (16, 18). Mouse embryos homozygous for K-*Ras* mutation die *in utero*, suggesting that K-*Ras* is essential for embryogenesis (33). Expression of Raf1 is recognized in various mouse fetal tissues (34). MEK1 and ERK are known to be necessary for PC12 cell neuronal differentiation (35, 36). These features suggest that Ras/MAPK signaling pathway plays a role in cellular regulation during developmental processes (34–36). Raf-1 expression has been detected at different stages of mouse tooth

Figure 4 Immunohistochemical reactivity for ERK1/2. (A) Tooth germ showing strong reactivity in inner and outer enamel epithelium and weak to moderate reactivity in stratum intermedium and stellate reticulum (×125). (B) Granular cell ameloblastoma showing marked reactivity in peripheral cuboidal cells and central polyhedral cells and decreased reactivity in granular cells (×95). (C) Ameloblastic carcinoma showing strong reactivity in most neoplastic cells (×115).

germ development (31), and ERK reactivity has been studied in odontogenic epithelial rests neighboring human odontogenic cysts (32). In the present study,

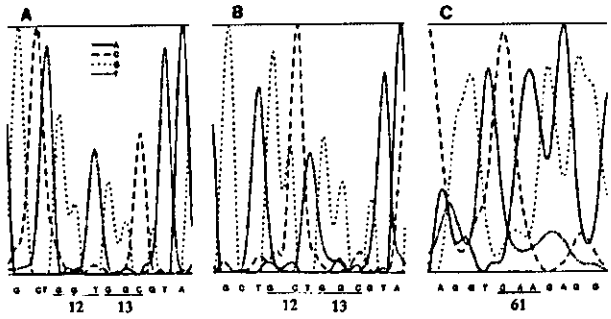

Figure 5 Direct DNA sequencing of K-*Ras* gene in ameloblastoma. (A) No mutation at codons 12 and 13 in exon 1. (B) A GGT to GCT point mutation at codon 12 in exon 1. (C) No mutation at codon 61 in exon 2.

Ras/MAPK signaling molecules were detected in epithelial components of tooth germs at the initial stage of crown mineralization. These features suggest that Ras signaling plays a role in cell proliferation and differentiation during tooth development.

Ras signaling functions as a relay switch in downstream of cell surface receptor tyrosine kinases, including receptors for many growth factors, such as epidermal (EGF), hepatocyte (HGF), platelet-derived (PDGF), insulin-like (IGF), fibroblast (FGF), vascular endothelial (VEGF), and nerve (NGF) growth factors (17, 18). Receptors for EGF, FGF, and HGF have been investigated in odontogenic tumors, suggesting that these receptor tyrosine kinases affect cell proliferation in oncogenesis or malignant transformation of odontogenic epithelium (29, 37–39). Aberrant expression and/or activation of signal transducing proteins are linked with neoplastic change (16, 20, 22). Alterations in Ras/MAPK signaling pathway, such as overexpression or constitutive activation of signaling molecules, have been detected in various malignancies, including lung, renal, prostate, breast, ovarian, and oral carcinomas (19, 21, 23, 40–42). Overexpression of $p21^{Ras}$ in ameloblastomas and activation of ERK in odontogenic cysts are related to the biological behavior of the odontogenic lesions (30, 32). In the present study, ameloblastomas expressed Ras/MAPK signaling molecules evidently in peripheral neoplastic cells, and basal cell ameloblastomas tended to show stronger reactivity for the signaling molecules than did the other subtypes. These features suggest that Ras/MAPK signaling pathway plays a role in promoting the proliferation of ameloblastoma cells. However, expression of Ras/MAPK signaling molecules in ameloblastomas did not clearly differ from that in tooth germs or malignant ameloblastomas. K-Ras immunoreactivity in malignant ameloblastomas was lower than that in dental lamina of tooth germs, whereas no apparent difference was found in reactivity for Raf1, MEK1, or ERK1/2 between tooth germs and malignant ameloblastomas. These results did not clearly show that these molecules have a specific role in oncogenesis or malignant transformation of odontogenic epithelium. In this study, expression of Ras/MAPK signaling molecules in plexiform ameloblastomas was slightly stronger than that in

follicular ameloblastomas. Keratinizing cells and granular cells showed decreased reactivity for the signaling molecules in acanthomatous and granular cell ameloblastomas. These features suggest that Ras/MAPK signaling might play a role in tissue structuring and/or cytodifferentiation of ameloblastomas.

A series of genetic alterations appear to promote the development of tumors via multiple steps (13, 43). Point mutations at codons 12, 13, and 61 of K-*Ras* gene are found in approximately 30% of solid tumors, and the incidences of these mutations are high in pancreatic, colorectal, lung, ovarian, and endometrial carcinomas (13, 14, 44–46). Mutated Ras product constitutively transduces signals and promotes cellular proliferation (10, 16). In the present study using direct DNA sequencing, a point mutation of K-*Ras* was detected at codon 12 in only 1 of 22 ameloblastomas and 1 metastasizing ameloblastoma, suggesting that K-*Ras* mutation might play a minor role in neoplastic change of odontogenic epithelium. Our immunohistochemical examination revealed relatively low reactivity for K-Ras product in ameloblastic carcinomas; however, mutation analysis of K-*Ras* gene in ameloblastic carcinomas could not be investigated because of the rarity of this malignancy. Further studies should be carried out to determine the association between K-*Ras* and the malignant potential of odontogenic epithelium.

References

1. Kramer IRH, Pindborg JJ, Shear M. *WHO Histological Typing of Odontogenic Tumours.* Berlin: Springer-Verlag, 1992; 11–27.
2. Melrose RJ. Benign epithelial odontogenic tumors. *Semin Diagn Pathol* 1999; **16**: 271–87.
3. Eversole LR. Malignant epithelial odontogenic tumors. *Semin Diagn Pathol* 1999; **16**: 317–24.
4. Sciubba JJ, Fantasia JE, Kahn LB. *Tumors and Cysts of the Jaw.* Washington, DC: Armed Forces institute of Pathology, 2001: 71–99.
5. Heikinheimo K, Jee KJ, Niini T, et al. Gene expression profiling of ameloblastoma and human tooth germ by means of a cDNA microarray. *J Dent Res* 2002; **81**: 525–30.
6. Jaakelainen K, Jee KJ, Leivo I, Saloniemi I, Knuutila S, Heikinheimo K. Cell proliferation and chromosomal changes in human ameloblastoma. *Cancer Genet Cytogenet* 2002; **136**: 31–7.
7. Shibata T, Nakata D, Chiba I, et al. Detection of TP53 mutation in ameloblastoma by the use of a yeast functional assay. *J Oral Pathol Med* 2002; **31**: 534–8.
8. Der CJ, Krontiris TG, Cooper GM. Transforming genes of human bladder and lung carcinoma cell lines are homologous to the *ras* genes of Harvey and Kirsten sarcoma viruses. *Proc Natl Acad Sci USA* 1982; **79**: 3637–40.
9. Shimizu K, Goldfarb M, Suard Y, et al. Three human transforming genes are related to the viral *ras* oncogenes. *Proc Natl Acad Sci USA* 1983; **80**: 2112–6.
10. Barbacid M. *ras* genes. *Ann Rev Biochem* 1987; **56**: 779–827.
11. Capon DJ, Seeburg PH, McGrath JP, et al. Activation of Ki-ras2 gene in human colon and lung carcinomas by two different point mutations. *Nature* 1983; **304**: 507–13.
12. Almoguera C, Shibata D, Forrester K, Martin J, Arnheim N, Perucho M. Most human carcinomas of the exocrine pancreas contain mutant c-K-*ras* genes. *Cell* 1988; **53**:549–54.
13. Vogelstein B, Fearon ER, Hamilton SR, et al. Genetic alterations during colorectal-tumor development. *N Engl J Med* 1988; **319**: 525–32.
14. Bos JL. *ras* oncogenes in human cancer: a review. *Cancer Res* 1989; **49**: 4682–9.
15. White MA, Nicolette C, Minden A, et al. *Cell* 1995; **80**: 533–41.
16. Seger R, Krebs EG. The MAPK signaling cascade. *FASEB J* 1995; **9**: 726–35.
17. Marshall CJ. Specificity of receptor tyrosine kinase signaling: transient versus sustained extracellular signal-regulated kinase activation. *Cell* 1995; **80**: 179–85.
18. Kolch W. Meaningful relationships. the regulation of the Ras/Raf/MEK/ERK pathway by protein interactions. *Biochem J* 2000; **351**: 289–305.
19. Hajj C, Akoum R, Bradley E, Paquin F, Ayoub J. DNA alterations at proto-oncogene loci and their clinical significance in operable non-small cell lung cancer. *Cancer* 1990; **66**: 733–9.
20. Gulbis B, Galand P. Immunodetection of the p21-*ras* products in human normal and preneoplastic tissues and solid tumors: a review. *Hum Pathol* 1993; **24**: 1271–85.
21. Oka H, Chatani Y, Hoshino R, et al. Constitutive activation of mitogen-activated protein (MAP) kinases in human renal cell carcinoma. *Cancer Res* 1995; **55**: 4182–7.
22. Hoshino R, Chatani Y, Tamori T, et al. Constitutive activation of the 41-/43-kDa mitogen-activated protein kinase signaling pathway in human tumors. *Oncogene* 1999; **18**: 813–22.
23. Albanell J, Codony-Sevat J, Rojo F, et al. Activated extracellular signal-regulated kinases: association with epidermal growth factor receptor/transforming growth factor α expression in head and heck squamous carcinoma and inhibition by anti-epidermal growth factor receptor treatments. *Cancer Res* 2001; **61**: 6500–10.
24. Kumamoto H. Detection of apoptosis-related factors and apoptotic cells in ameloblastomas. analysis by immunohistochemistry and an in situ DNA nick end-labelling method. *J Oral Pathol Med* 1997; **26**: 419–25.
25. Kumamoto H, Ooya K. Immunohistochemical analysis of bcl-2 family proteins in benign and malignant ameloblastomas. *J Oral Pathol Med* 1999; **28**: 343–9.
26. Kumamoto H, Kimi K, Ooya K. Immunohistochemical analysis of apoptosis-related factors (Fas, Fas ligand, caspase-3 and single-stranded DNA) in ameloblastomas. *J Oral Pathol Med* 2001; **30**: 596–602.
27. Kumamoto H, Kinouchi Y, Ooya K. Telomerase activity and telomerase reverse transcriptase (TERT) expression in ameloblastomas. *J Oral Pathol Med* 2001; **30**: 231–6.
28. Kumamoto H, Kimi K, Ooya K. Detection of cell cycle-related factors in ameloblastomas. *J Oral Pathol Med* 2001; **30**: 309–15.
29. Kumamoto H, Yoshida M, Ooya K. Immunohistochemical detection of hepatocyte growth factor, transforming growth factor-β and their receptors in epithelial odontogenic tumors. *J Oral Pathol Med* 2002; **31**: 539–48.
30. Sandros J, Heikinheimo K, Happonen R-P, Stenman G. Expression of p21RAS in odontogenic tumors. *APMIS* 1991; **99**: 15–20.
31. Sunohara M, Tanzawa H, Kaneko Y, Fuse A, Sato K. Expression patterns of Raf-1 suggest multiple roles in tooth development. *Calcif Tissue Int* 1996; **58**: 60–4.
32. Nickolaychuk B, McNicol A, Gilchrist J, Birek C. Evidence for a role of mitogen-activated protein kinases in proliferating and differentiating odontogenic epithelia

of inflammatory and developmental cysts. *Oral Surg Oral Med Oral Pathol Oral Radiol Endod* 2002; **93**: 720–9.
33. Johnson L, Greenbaum D, Cichowski K, et al. K-*ras* is an essential gene in the mouse with partial functional overlap with N-*ras*. *Genes Dev* 1997; **11**: 2468–81.
34. Storm SM, Cleveland JL, Rapp UR. Expression of *raf* family proto-oncogenes in normal mouse tissues. *Oncogene* 1990; **5**: 345–51.
35. Qui M-S, Green SH. PC12 cell neuronal differentiation is associated with prolonged $p21^{ras}$ activity and consequent prolonged ERK activity. *Neuron* 1992; **9**: 705–17.
36. Cowley S, Paterson H, Kemp P, Marchall C. Activation of MAP kinase kinase is necessary and sufficient for PC12 differentiation and for transformation of NIH 3T3 cells. *Cell* 1994; **77**: 841–52.
37. Shrestha P, Yamada K, Higashiyama H, Takagi H, Mori M. Epidermal growth factor receptor in odontogenic cysts and tumors. *J Oral Pathol Med* 1992; **21**: 314–7.
38. Heikinheimo K, Voutilainen R, Happonen R-P, Miettinen PJ. EGF receptor and its ligands, EGF and TGF-α, in developing and neoplastic human odontogenic tissues. *Int J Dev Biol* 1993; **37**: 387–96.
39. So F, Daley TD, Jackson L, Wysocki GP. Immunohistochemical localization of fibroblast growth factors FGF-1 and FGF-2, and receptors FGFR2 and FGFR3 in the epithelium of human odontogenic cysts and tumors. *J Oral Pathol Med* 2001; **30**: 428–33.
40. Sivaraman VS, Wang H-Y, Nuovo GJ, Malbon CC. Hyperexpression of mitogen-activated protein kinase in human breast cancer. *J Clin Invest* 1997; **99**: 1478–83.
41. Magi-Galluzzi C, Mishra R, Fiorentino M, et al. Mitogen-activated protein kinase phosphatase 1 is overexpressed in prostate cancers and is inversely relate to apoptosis. *Laboratory Invest* 1997; **76**: 37–51.
42. Kupryjanczyk J, Szymanska T, Madry R, et al. Evaluation of clinical significance of TP53, BCL-2, BAX and MEK1 expression in 229 ovarian carcinomas treated with platinum-based regimen. *Br J Cancer* 2003; **88**: 848–54.
43. Fearon ER, Vogelstein. A genetic model for colorectal tumorigenesis. *Cell* 1990; **61**: 759–67.
44. Forrester K, Almoguera C, Han K, Grizzle WE, Peruch M. Detection of high incidence of K-*ras* oncogenes during human colon tumorigenesis. *Nature* 1987; **327**: 298–303.
45. Enomoto T, Weghorst CM, Inoue M, Tanizawa O, Rice JM. K-*ras* activation occurs frequently in mucinous adenocarcinomas and rarely in other common epithelial tumors of the human ovary. *Am J Pathol* 1991; **139**: 777–85.
46. Imamura T, Arima T, Kato H, Miyamoto S, Sasazuki T, Wake N. Chromosomal deletions and K-*ras* gene mutations in human endometrial carcinomas. *Int J Cancer* 1992; **51**: 47–52.

Original Paper

Caries Research

Caries Res 2004;38:448–453
DOI: 10.1159/000079626

Received: April 2, 2003
Accepted after revision: November 25, 2003

A Method for Mapping the Distribution Pattern of Cariogenic Streptococci within Dental Plaque in vivo

K. Kato[a] T. Sato[b] N. Takahashi[b] K. Fukui[a] K. Yamamoto[a] H. Nakagaki[a]

[a]Department of Preventive Dentistry and Dental Public Health, School of Dentistry, Aichi-Gakuin University, Nagoya, and [b]Division of Oral Ecology and Biochemistry, Department of Oral Biology, Tohoku University Graduate School of Dentistry, Sendai, Japan

Key Words

Dental plaque · Distribution of microorganisms · Nested polymerase chain reaction · *Streptococcus mutans* · *Streptococcus sobrinus*

Abstract

This study was carried out to develop a method for mapping the distribution of cariogenic oral streptococci, *Streptococcus mutans* and *Streptococcus sobrinus*, from the outermost to the innermost plaque. Ten consenting subjects were asked to form plaque by abstaining from tooth brushing over 3 days within in situ plaque-generating devices, which were placed on the upper molars. The plaque formed in the devices was separated into 8–10 layered fractions (100 μm thick). Genomic DNA was extracted from each plaque fraction by a commercial DNA purification kit and used for the amplification of the 16S ribosomal RNA gene sequences by polymerase chain reaction (PCR) with universal primers. The products were then amplified by PCR with *S. mutans*- or *S. sobrinus*-specific nested primers. The final products were separated on agarose gels, stained and photographed to confirm the existence of *S. mutans* and *S. sobrinus*. The results showed that *S. mutans* was detected in the plaque obtained from all of the 10 subjects and *S. sobrinus* in the plaque of 7 subjects. However, the distribution patterns of fractions positive for *S. mutans* and *S. sobrinus* varied among the subjects, with a tendency for frequent detection of both species in the outer to middle layers of dental plaque. There were no plaque fractions in which only *S. sobrinus* was found. This method could be useful to map the distribution of cariogenic microorganisms and to estimate the bacterial ecology for oral biofilm.

Dental plaque is the tooth-associated biofilm consisting of a microbial community and a matrix of polymer of bacterial and host origin, and is also found on the various restorative materials introduced by dental treatment. Dental plaque plays a primary role in the etiology of dental caries, so their biological and cariogenic properties are basic to caries prevention. Mutans streptococci including *Streptococcus mutans* and *Streptococcus sobrinus* have been well known as the group of oral microorganisms which have virulence factors related to cariogenicity. They drop the plaque pH to low levels by producing acids from carbohydrates and survive in this acidic environment. They also produce extracellular polysaccharides which may promote the dissolution of the tooth surfaces by increasing the porosity of plaque matrix and permitting deeper penetration of sugar [Dibdin and Shellis, 1988; Cury et al., 2000]. Epidemiological studies have provided strong evidence of the relationship between the levels of mutans streptococci and the development of caries [Lang et al., 1987; Roeters et al., 1995]. In addition,

KARGER
Fax + 41 61 306 12 34
E-Mail karger@karger.ch
www.karger.com

0008–6568/04/0385–0448$21.00/0

Accessible online at:
www.karger.com/cre

Dr. Kazuo Kato, Department of Preventive Dentistry and
Dental Public Health, School of Dentistry, Aichi-Gakuin University
1-100 Kusumoto-cho, Chikusa-ku, Nagoya 464-8650 (Japan)
Tel. +81 52 751 2561, ext. 352, Fax +81 52 752 5988
E-Mail kazkato@dpc.aichi-gakuin.ac.jp

their early acquisition by children is positively correlated with white spot lesions or lesions with cavitation [Köhler et al., 1988; Caufield et al., 1993; Milgrom et al., 2000]. Therefore, the levels of mutans streptococci in plaque [Milgrom et al., 2000; Pienihäkkinen and Jokela, 2002] and saliva [Jensen and Bratthall, 1989] are considered to be important indicators for assessment of caries risk or management of caries prevention.

Dental plaque is a watery and frail heterogeneous complex material accumulating on the teeth. As dental plaque accumulates and matures, the depth-specific microbial differences in dental plaque may increase, depending on several physiological factors such as the oxygen concentration, pH, and nutrient availability. However, little attention has been paid to the detection or the identification of plaque bacteria relating to the structure of plaque on the tooth surface.

Several attempts have been made to clarify the location of specific bacteria in plaque. Ritz [1969] applied immunofluorescent staining of plaque sections to demonstrate the spatial relationship between aerobic and anaerobic bacteria in the plaque. This technique has often been used to detect periodontal pathogens in the apical plaque border [Christersson et al., 1987]. Noiri et al. [2001] found periodontal disease-associated bacteria in the periodontal tissue surrounding the roots of teeth that were extracted from periodontitis patients. Recently, a confocal laser scanning microscope (CLSM) has also been applied to study the relationship between the spatial structure of smooth surface plaque and the microbial ecology [Wood et al., 2000; Auschill et al., 2001].

We have reported on the fluoride and mineral profiles of the plaque formed in an in situ plaque-generating device after the exposure to fluoride solutions, using layer-specific analysis [Kato et al., 1997, 2002]. This technique enables us to analyze the distribution of specific materials such as cariogenic bacteria in the dental plaque structure. The aim of this study was to develop a method which could clarify the distribution pattern of cariogenic oral streptococci, *S. mutans* and *S. sobrinus*, throughout the plaque grown on an in situ device placed on the specific tooth site.

Materials and Methods

Plaque Sampling

In situ plaque-generating devices containing plaque receptacles (2 mm in diameter and 0.8–1 mm deep) were made by attaching nylon rings to autoclaved natural enamel slabs [Robinson et al., 1997]. Ten consenting healthy volunteers, 5 males and 5 females, 21–45 years of age, wore these sampling devices to collect plaque from either the upper left or upper right dental arch, using a custom-made dental alloy clasp, as previously reported [Kato et al., 1997]. The subjects were advised to use nonfluoridated toothpaste from at least 1 week before the plaque collection, avoiding rinsing with therapeutic mouthwash. They were asked to form plaque within the devices by abstaining from tooth brushing or by removing the appliances for oral hygiene without toothpaste, after which they were replaced at the same site. After a plaque formation period lasting for 3 days, the devices on the clasps were collected for analysis at least 1 h after any food or drink intake. The DMFS scores were also recorded by oral examination. The experimental design was approved by the Ethics Committee of Aichi-Gakuin University.

Plaque Sample Preparation

The devices, removed from the mouth, were snap-frozen in liquid nitrogen and freeze-dried overnight. They were then impregnated with a mixture of 10% methyl and 90% *n*-butyl methacrylate (Sigma Chemical, St. Louis, Mo., USA). Series of plaque sections parallel to the tooth surface (containing 4 sections of 4 μm thickness and 2 sections of 2 μm thickness; total 20 μm thickness) were repeatedly cut from the outer plaque surface towards the enamel surface, using an ultramicrotome (Ultrotome, LKB, Sweden). Sectioning continued until no sample remained. Each plaque sample was separated into several (8–10) sequential 100-μm-thick specimens consisting of five sets of serial sections (i.e. 20 μm × 5) using this procedure.

Out of the series of plaque sections, 2-μm-thick sections were spread on a glass slide, stained with a 0.05% neutral toluidine blue solution and used to check the presence of plaque. Five series of thicker sections were combined in sequential order and placed in a 0.5-ml sterilized polypropylene tube. Then, chloroform (200 μl) was poured into each tube to dissolve the polymer infiltrated into the specimen. After evaporation, the plaque specimen remained at the bottom of the tube. The preparation of the plaque samples is shown in figure 1.

PCR Analysis

200 μl of the InstaGene Matrix Kit (Bio-Rad Laboratories, Richmond, Calif., USA) was added to each tube. Genomic DNA was extracted from the plaque fraction according to the manufacturer's instructions. The 16S rRNA gene sequences were amplified by PCR with universal primers: 8UA and 1492R [Sato et al., 1997] and *Taq* DNA polymerase (HotStarTaq Master Mix, Qiagen GmbH, Hilden, Germany) according to the manufacturer's instructions. The primer sequences were: 8UA, 5′-AGA GTT TGA TCC TGG CTC AG-3′; and 1492R, 5′-TAC GGG TAC CTT GTT ACG ACT T-3′. PCR amplification was performed in a PCR Thermal Cycler MP (TaKaRa Biomedicals, Ohtsu, Shiga, Japan) programmed for 15 min at 95°C for initial heat activation and 35 cycles of 1 min at 94°C for denaturation, 1 min at 55°C for annealing, and 1.5 min at 72°C for extension, followed by 10 min at 72°C for a final extension. The predicted PCR product with the universal primers was 1,505 bp in length.

Then the PCR products were amplified by the species-specific PCR based on the 16S rRNA gene sequences [Rupf et al., 2001] with *S. mutans*-specific primers sm1 and sm2, and with *S. sobrinus*-specific primers SobF and SobR. The nested primer sequences were as follows: *S. mutans*-forward primer (sm1), 5′-GGT CAG GAA AGT CTG GAG TAA AAG GCT A-3′; *S. mutans*-reverse primer (sm2), 5′-GCG TTA GCT CCG GCA CTA AGC C-3′; *S. sobrinus*-forward primer (SobF), 5′-CGG ACT TGC TCC AGT GTT ACT AA-3′; and

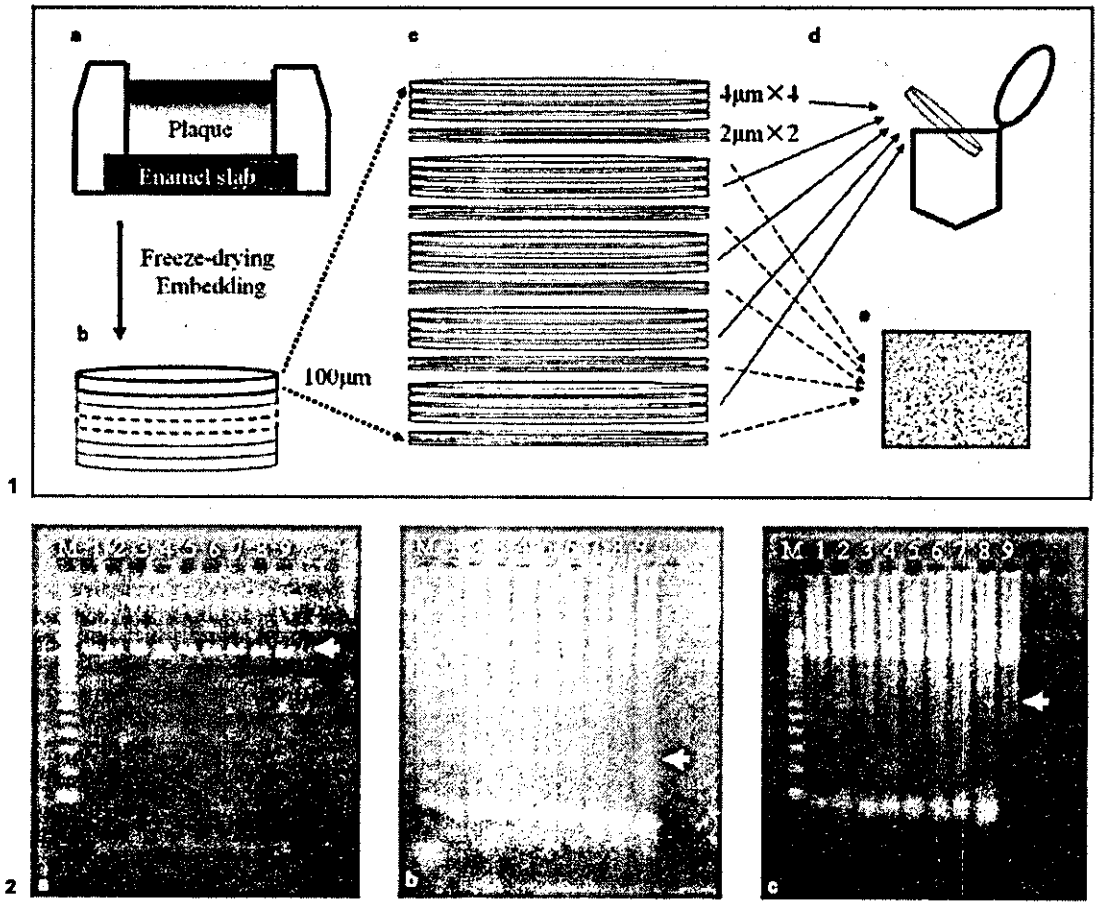

Fig. 1. **a** Plaque in the plaque-generating device. **b** Arrangement of 100-μm-thick layers in the plaque sample. **c** Sectioning process for obtaining one layer. **d** Collection of thicker sections for nested PCR analysis. **e** Optical observation of stained thinner sections.

Fig. 2. Detection of 16S rRNA gene amplified by PCR with universal primers (**a**) and the PCR products amplified by *S. mutans*-specific (**b**) and *S. sobrinus*-specific (**c**) nested primers. Positive bands are indicated with arrows. A sample taken from subject F was divided into 8 layers. M indicates 100-bp DNA markers. Lanes 1 and 8 are the outermost (1st) and the innermost (8th) layers, respectively. Lane 9 is a blank control without plaque fragments.

S. sobrinus-reverse primer (SobR), 5′-GCC TTT AAC TTC AGA CTT AC-3′. PCR amplification was carried out as previously described. The sizes of the expected PCR products of *S. mutans* and *S. sobrinus* were 282 and 546 bp, respectively.

PCR products were separated on 2% agarose gels using electrophoresis in TBE buffer (100 m*M* Tris, 90 m*M* boric acid, 1 m*M* EDTA, pH 8.4), stained with ethidium bromide and photographed under UV light. A 100-bp DNA ladder (Invitrogen Corp., Carlsbad, Calif., USA) was used as the molecular size marker.

Blank control without any plaque fragments was prepared in order to check the extraction of genomic DNA from the specimen and the presence of contamination. An example of the procedure used on cariogenic bacteria from the gel is shown in figure 2.

Results

S. mutans were detected in the plaque taken from all of the 10 subjects, and *S. sobrinus* in the plaque of 7 of the subjects (table 1). However, both strains were not always detected in every layer of the plaque, although both were found throughout the plaque taken from 1 participant (subject D). These positive layers were also recognized continuously, although the layers containing *S. mutans* were dispersed in the plaque taken from subjects B, G and I. The proportions of layers in which *S. mutans* and *S. so-*